

Physicochemical Characteristics of Waste Sea Shells for Acid Gas Cleaning Absorbent

Jong Hyeon Jung, Byung Hyun Shon*, Kyung Sun Yoo** and Kwang Joong Oh***†

Dept. of Environmental Engineering, Sorabol College, 165 Chung-hyo dong, Kyong-ju,
Kyungbuk 780-711, Korea

*Dept. of Environmental Engineering, Hanseo University, Hae-mi myun, Seosan,
Chung-nam 356-820, Korea

**Dept. of Environmental Engineering, Kawngwoon University, Wolke-Dong,
Noweon Gu, Seoul 139-701, Korea

***Dept. of Environmental Engineering, Pusan National University, San 30,
Changjeon-Dong, Kumjeong-Gu, Pusan 609-735, Korea

(Received 18 May 2000 • accepted 15 August 2000)

Abstract—The properties of waste shells, which cause pollution problems, are investigated in Southern beach, Korea. The absorbent surface area was affected by the contaminant gas removal efficiency of the waste shell absorbents, pore structures, absorbent deliquescence and hygroscopicity during the contaminant gas reaction. The BET surface area of calcination/hydration waste shell and limestone samples was increased by hydration in isothermal conditions. The absorption rate with acid gas is predicted by apparatus for measuring the hydration rate. The BET surface area of waste shell samples hydrated at 90 °C isothermal condition was greatly increased. And pore size distribution and diameter were increased after calcination/hydration reaction. Waste seashells can be regarded as a good absorbent for removing acid gases. Therefore, the recycling of waste seashells as a substitute for limestone would be profitable.

Key words: Waste Shell, Absorbent, Hydration Rate, Flue Gas Desulfurization

INTRODUCTION

Air pollution problems due to the emission of air pollutants from various industrial facilities have become a serious issue and numerous air pollution processes have been developed [Acharya, 1991; Dempsey, 1993; KIER, 1996]. It is well known that alkali absorbents such as CaO , CaCO_3 and $\text{Ca}(\text{OH})_2$ are used to remove SO_2 and/or HCl in flue gas cleaning processes [Karlsson, 1981; Brian, 1992; Jozewicz, 1988, 1994]. These absorbents show good reactivity toward acidic gases and lower cost compared to other metal oxide absorbents [David, 1981; Jozewicz, 1987, 1989]. Recently, a large amount of oyster shells have accumulated around the South Sea and caused a notorious smell during the summer season. It should be also noted that these shells, one of the most representative sea wastes, consist of pure CaCO_3 with couples of thin membrane and SiO_2 . A few researches are being carried out to develop these waste shells as a material for cleaning industrial wastewater. These researches make it possible to remove water pollution problems by using solid waste recycling technology. Therefore, the feasibility of using waste shells as acid gas cleaning absorbents needs to be investigated.

The objective of this study is to develop an absorbent of waste shells, which can remove gaseous acid pollutants emitted from the

incinerator and power plants [Frame, 1988]. The effects of hydration conditions of waste shells on the physicochemical characteristics have been investigated by using several instruments, and a desulfurization reaction activity test of waste shell absorbent was carried out in a fixed bed reactor.

MATERIALS AND METHODS

The seashells of oyster, hard-shelled mussels, clams and seashells from Tong Young province around the South Sea were used as a main material. Salts and other organic substances were removed by washing and drying the waste seashells. Limestone from Danyang province was adapted for comparison of physicochemical properties of waste seashells. All the materials were crushed 2 times by a Jaw crusher and Ball mill after sufficient drying. The physical and chemical characteristics of the waste shell absorbent were analyzed by ICP (ICPS-7500 Shimadzu, Japan), SEM (JEOL superprobe JSM-5400, USA), XRD (SIMENS, Deutsche), and BET (Micromeritics Co., USA). ICP was applied to analyze the atomic properties of the materials [Weast, 1985]. SEM was used to observe the microstructure of the surface of wasted shells. Surface area of the absorbent was measured by BET technique after pre-treating to remove vapor in vacuum 1×10^{-3} and 180 °C for 2 hours. The crystal state of shell absorbent and the products before and after reaction was assured by X-ray diffractometer under the condition of 30 kV and 20 mA in the range of 10-70 degrees.

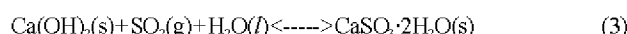
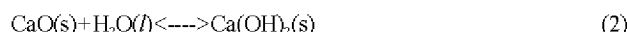
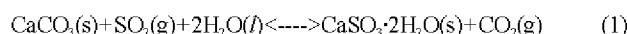
The hydration apparatus was manufactured in order to investigate the effects of properties of calcination absorbent and hydration condition on the reactivity of the hydrated lime [EPRI, 1988]. The

†To whom correspondence should be addressed.

E-mail: kjoh@hyowon.cc.pusan.ac.kr

This paper was presented at The 5th International Symposium on Separation Technology-Korea and Japan held at Seoul between August 19 and 21, 1999.

reactivity of calcined waste shell was compared with that of imported lime samples. Also, the hydration state according to initial temperature was confirmed. These were conducted by measuring the reactivity of quicklime. The samples were placed in a stirred vacuum flask containing deionized water, and the temperature was measured at time intervals. Rate of heat release was a measure of reactivity. The faster the temperature increases, the faster the slaking rate. This method can be used in flasker design, to improve slaker performance, to evaluate and compare different limes, or test incoming lime shipments for quality control purposes. A more reactive lime will require a shorter residence time or smaller slaker volume than a less reactive lime [EPRI, 1988]. Combining the following equation can derive the overall reactions of each absorbent with SO_2 [Nakamura, 1995; Ronald, 1995; Paolo, 1995].



It was calculated for the hydration speed to measure the hydrated reaction using the device of Fig. 1 with calcined shell absorbents suggested by EPRI [1988], respectively. This device was designed to react under the same temperature according to the change of hydration conditions and consisted of a Dewar flask wrapped dual rubber plate and a mixer made with tepron. A K-type thermocouple (1/8", 30 cm) and a thermoscope were installed on the upper side of the flask and confirmed the variation of inner temperature. In order to check hydration rate, the crushed seashells sieved with the degree of 6 mesh was adapted to the calcination reaction. To the Dewar flask was added 900 ml water of 25 °C. And a mixer was set to 400 rpm [EPRI, 1988]. After CaO (100 g) was fed, the data system was continuously operated to check the temperature variation every 5 seconds.

The schematic diagram of the gas removal experiment is shown

in Fig. 2. A fixed type reactor to check the reaction of flue gas was installed in the air bath and it was 25 mm width and 250 mm-height stainless steel pan [Robert, 1992; Ronald, 1995; Krammer, 1997]. A metal filter was on the 150-mm height from its bottom, and then the experimental material was put on this filter under regular temperature. The temperature of the air bath was in the range of 0-300 °C under ±1 °C. When the absorbents were put in the reactor, simulated-gas would be injected and reacted gas was supposed to be spouted. The system consisted of a simulated-gas injection part, reactor part, reacted gas analysis and data check part. The gas injected by MFC to reactor was simulated-gas consisting of SO_2 and N_2 , and the total injection amount was 3.0 L/min. The water was injected by syringe pump to keep the same humidity and was supplied steam passing through the steam maker under 180 °C. To check the water balance in the reactor, a Thermos Hygrometer was installed in the outlet where the steam goes out and the area was sealed with heating tape to prevent the gas from being condensed by decreasing temperature. This was because the air was eliminated by hydration and dust passing through a cooling condenser and reactor filled with CaSO_4 . Since hydration was eliminated two times, fixed flow was supplied through a flow meter installed in the inlet. The gas injected to the reactor and SO_2 after reaction was checked continuously and analyzed by IR type SO_2 Analyzer.

Packing an absorbent to the reactor, absorbent 1 g and quartz stand 19 g were mixed to prevent the experimental material from being condensed and to ensure the gas flow could be smooth when the absorbents were injected to the reactor. Once the experimental material was put into reactor, the air oven was kept under the same temperature. Then, hydrogen and nitrogen were injected to eliminate oxygen in the absorbents for 10 minutes and to keep the simulated-gas and humidity regular. Then the valve was switched to the bypass line and the thickness of each gas was balanced with the injection of other gas including SO_2 . When the thickness of

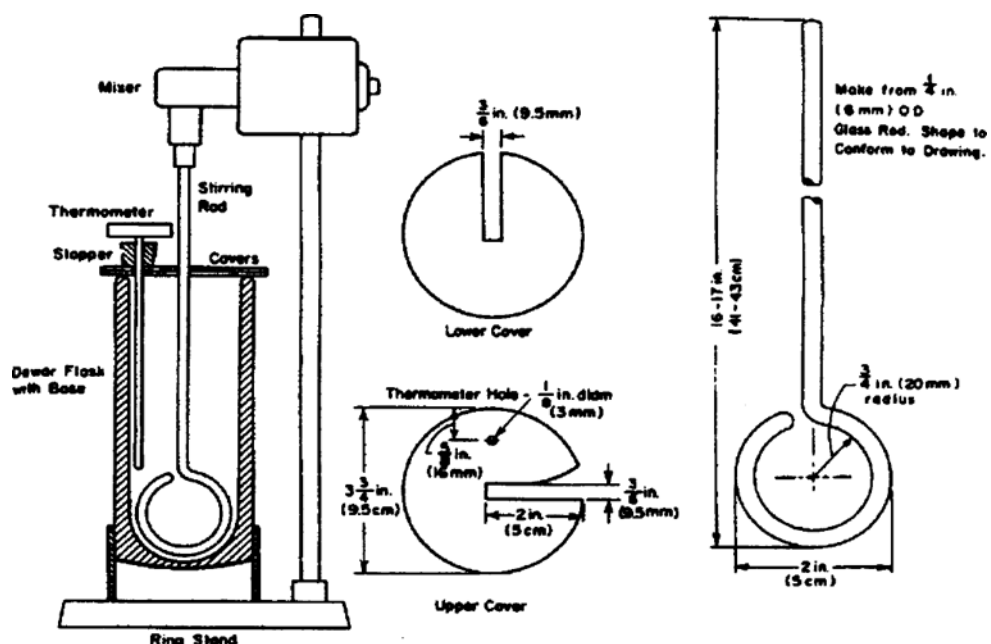


Fig. 1. Experimental apparatus for measuring the hydration rate of absorbents.

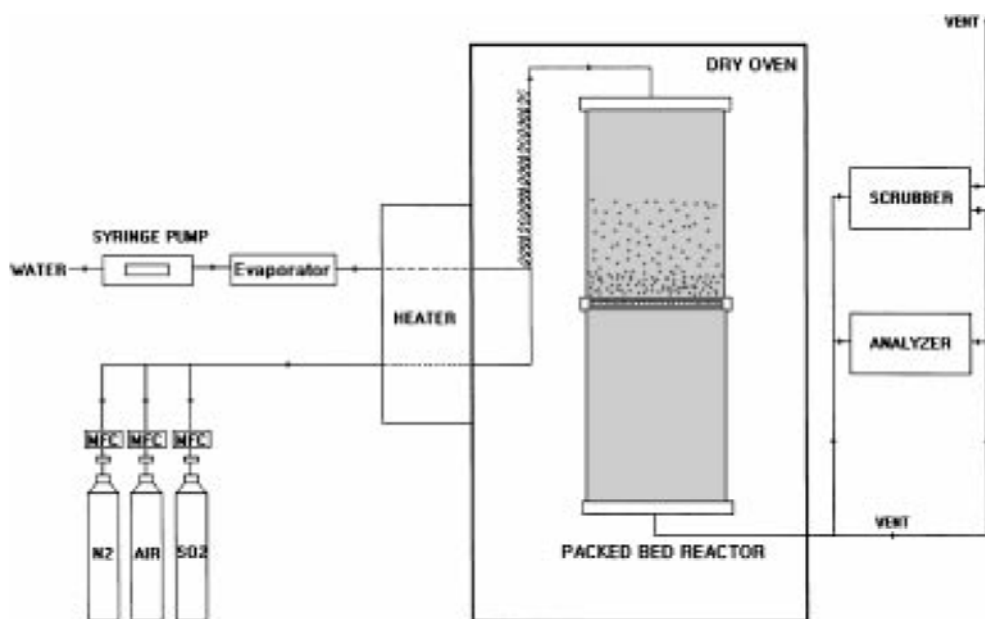


Fig. 2. Schematic diagram of desulfurization experimental apparatus.

simulated gas was fixed regularly, the bypass line valve was turned the switch to the reactor and the experiment was actually commenced.

The real-time data system was used to show the reaction according to the change of temperature. RSC232 Port transferred the real-time data to a 486-DX Computer, since recording continuously the electric signal generated from the measuring instrument with Hybrid Recorder.

RESULTS AND DISCUSSION

Fig. 3 shows the results of XRD analyses of limestone and oyster shell with and without calcination. As can be seen in Fig. 3A, maximum peaks appear at around a 2θ value of 29.4, which can be assigned to limestone. The peaks of CaCO_3 also appear at around the 2θ values of 39, 43, and 48. Fig. 3C shows XRD results of calcined materials at around the 2θ values of 37 and 54. The intensity of these peaks increases with increasing the calcination temperature, indicating a CaO phase has been formed enough after calcination followed by hydration reaction. Comparing the results of Fig. 3 with Table 1, we can see that the waste seashells (oyster, hard-shelled mussel, clam, and seashell) can be utilized as FGD absorbent.

Fig. 4 shows the change of specific surface area of calcined hydration limestone. As shown in Fig. 4a, specific surface area of calcined hydration limestone particles increases rapidly with increasing hydration time up to 6 hours and then slowly increases to 12 m^2/g . Effects of hydration temperature on the specific surface area of the calcined limestone are shown in Fig. 4b. When the initial water temperature was in the range of 30-90 °C with every 10 °C, up to the 70 °C BET surface area was not changed largely. However, a rapid increase of BET surface area of absorbent appears above the temperature of 80 °C, indicating that a rapid hydration reaction occurs. We can conclude that the optimum range of temperature and time for hydration reaction of absorbent is about 80-

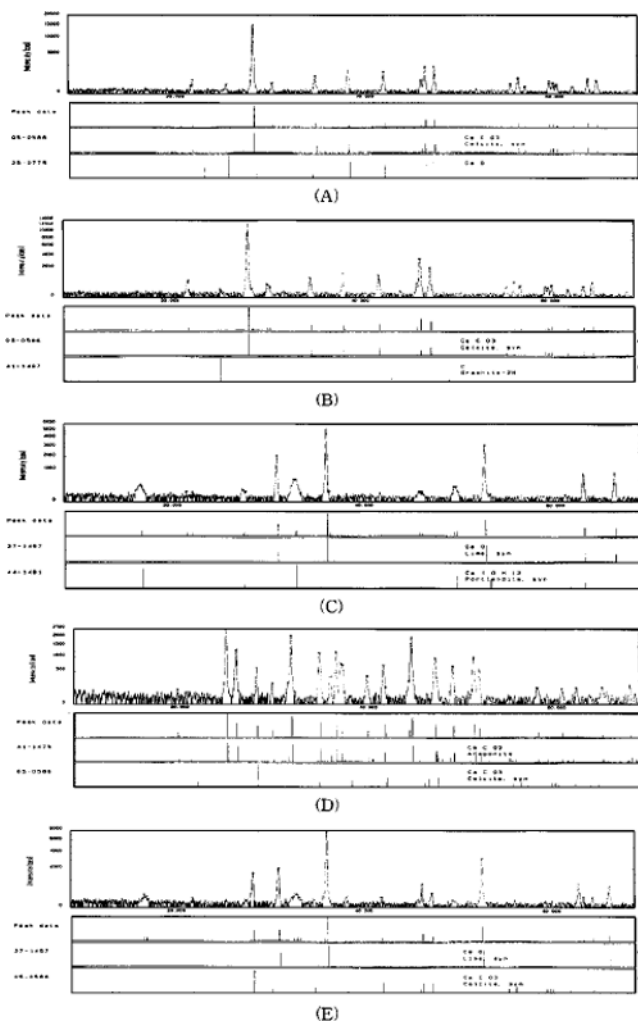


Fig. 3. XRD results of various absorbents.

(A) limestone, (B) oyster, (C) calcined oyster, (D) clam, and (E) calcined clam.

Table 1. Analysis of oyster, hard shelled mussel, clam, seashell (wt%)

Components		SiO ₂	Al ₂ O ₃	Fe ₂ O ₃	CaO	MgO	Igloss
Contents (%)	Oyster	0.40	0.22	0.04	53.81	0.70	44.87
	Hard-shelled mussel	0.20	0.13	0.03	53.70	0.33	45.61
	Clam	0.46	0.20	0.04	53.92	0.22	45.16
	Seashell	0.66	0.40	0.04	53.58	0.20	45.12

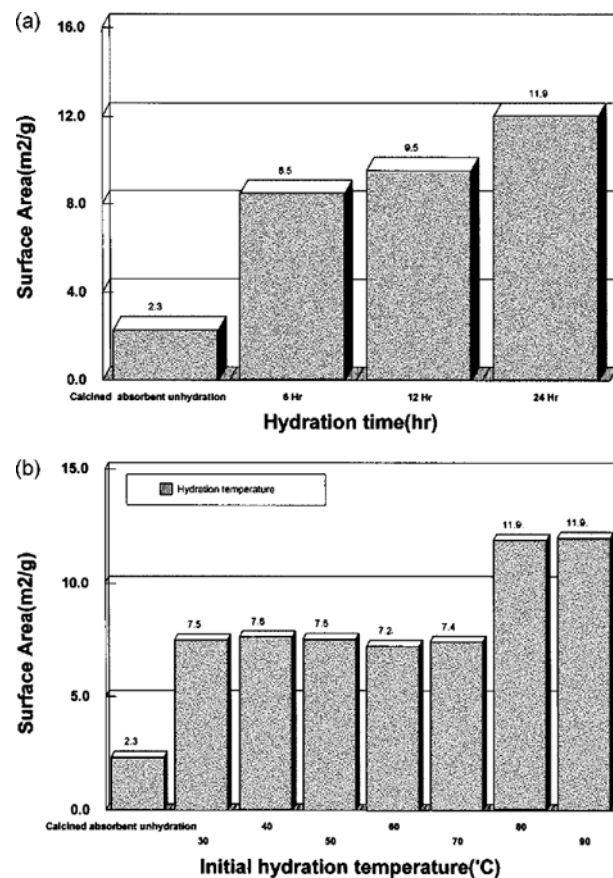


Fig. 4. (a) Variation of surface area of calcined limestone as a function of hydration time. (b) Effect of hydration temperature on the surface areas of calcined limestone.

90 °C and 24 hours, respectively.

Fig. 5A-E shows BET results for oysters, hard-shelled mussels, clams, and seashells. This figure shows the difference of amount of nitrogen gas according to the change of relative pressure absorbed to waste shell and limestone. We can conclude that each of the absorbents shows a similar BET value in the condition of raw material. Fig. 5F shows pore size distribution of limestone, oyster, hard-shelled mussel, clam, and seashell according to pore diameter. The results lead to the finding that shells have larger average pore size with the value of pore volume of 0.013-0.024 cm³/g, which is higher than that of limestone.

Fig. 6A is pore size distribution of the samples with a variation of pore diameter before and after calcination. Fig. 6B also shows pore size distribution of limestone before and after hydration. Fig. 6C is pore size distribution according to the change of pore diameter of limestone manufactured as an absorbent with calcination and hydration. It appeared that the average pore diameter of limestone

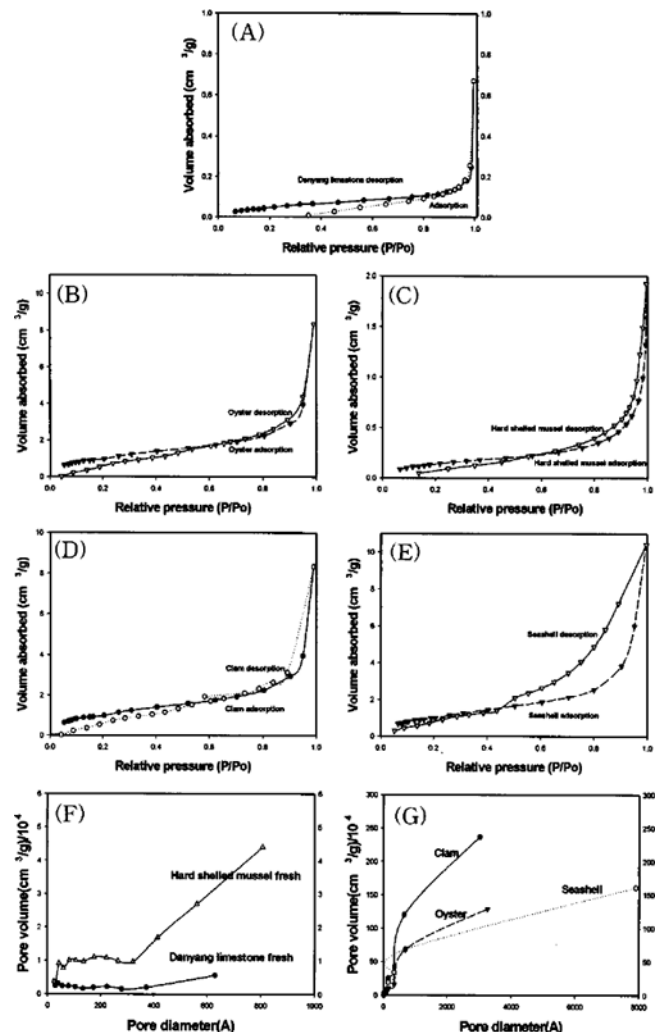


Fig. 5. N₂ BET results of various waste seashells and limestone.

(A) fresh limestone, (B) fresh oyster, (C) fresh hard-shelled mussel, (D) fresh clam, (E) fresh seashell, (F) fresh limestone and hard shelled mussel (G) fresh clam, seashell, oyster.

was much bigger than that of the raw materials. This result also indicates that calcination and hydration processes can enhance the removal capacity of acid gases.

Fig. 7 shows the SEM photographs of the fresh limestone, hydrated limestone, calcined limestone and hydration/calcinations limestone sample. Fig. 7A shows 3500 magnifications after filtering and sieving with 40/60 mesh. Fig. 7B is for calcined material and Fig. 7C for calcined material and Fig. 7D for limestone after calcination/hydration sample. The specific surface area of low limestone is very small since it consists of inorganic materials without pores in compacted components, but Fig. 7C shows many micro-

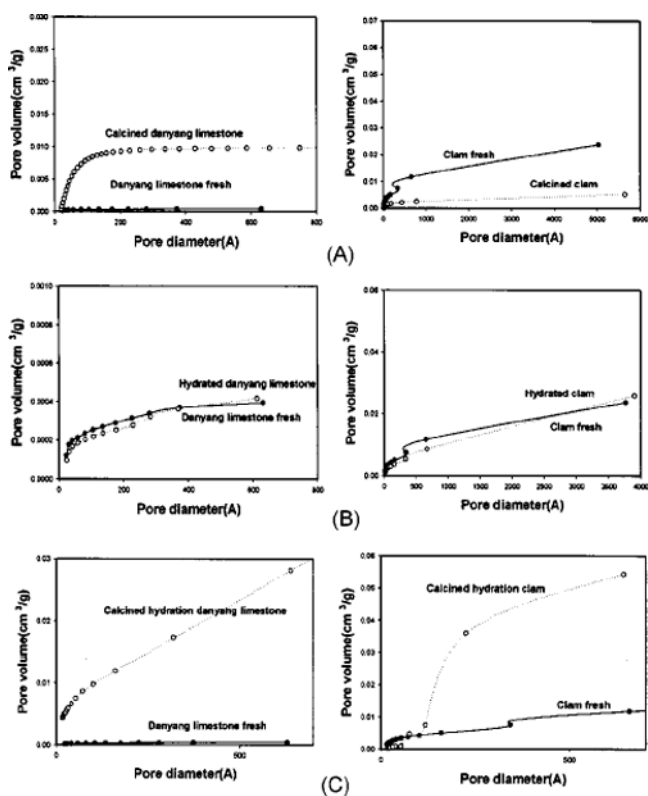


Fig. 6. N_2 BET results of limestone and clam with a variation of pretreatment condition.

(A) fresh limestone and clam, (B) calcined limestone and clam
(C) hydrated after calcination of limestone and clam.

pores formed because of the evolution of CO_2 gas producing CaO phase in the limestone particles. Fig. 7D shows small pores are formed in the surface texture of limestone particles after calcination/hydration. This result leads to the following conclusion that surface area is enhanced by the hydration reaction.

Fig. 8 shows raw particle sample condition, hydration, calcinations, calcinations and hydration reaction clam sample by SEM. (A) for filtered condition of clams, (B) for calcinated material, (C) for calcinated material, (D) for calcinated and hydrated clams. (A) shows small specific surface condition with tight structure while (C) shows decreased specific surface area by SEM analysis if calcinated. This decrease was affected by deformation of pores, which is caused from calcination of micropore while low limestone showed the increased specific surface area could be reacting with gas. Moreover, (D) shows the particles of calcinated/hydrated clam shells are more increased in specific surface area than the calcinated particles, and BET specific surface area before/after hydration is highly increased. In addition, pore distribution and pore diameter are highly increased as well. The calcination/hydration reaction is considered to improve the ability of absorption and adsorption properties for detach of acidic gas. In case of clamshells, pore size distribution was $0.1025\text{ m}^2/\text{g}$ and increased more than 20 times before calcination.

Fig. 9 shows the variation of hydration temperature of the calcined samples as a function of hydration reaction time. In the case of raw limestone, which has high reaction activity, by-products are considerably expected to reduce due to decreased retention time in

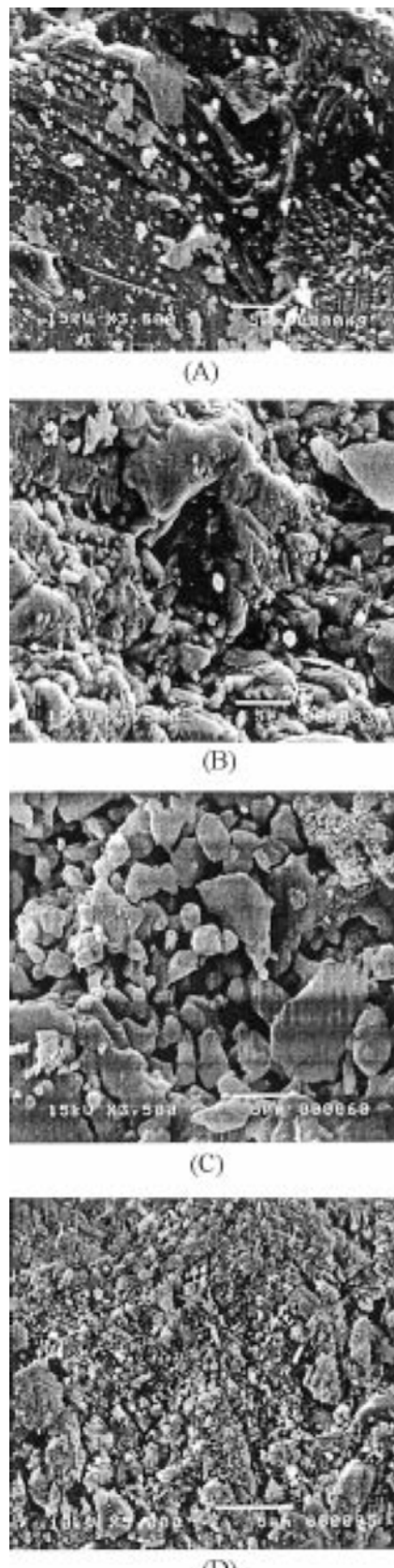


Fig. 7. SEM photographs of limestone with a variation of pre-treatment condition.

(A) fresh limestone, (B) hydrated limestone, (C) calcined limestone, (D) hydrated after calcination of limestone.

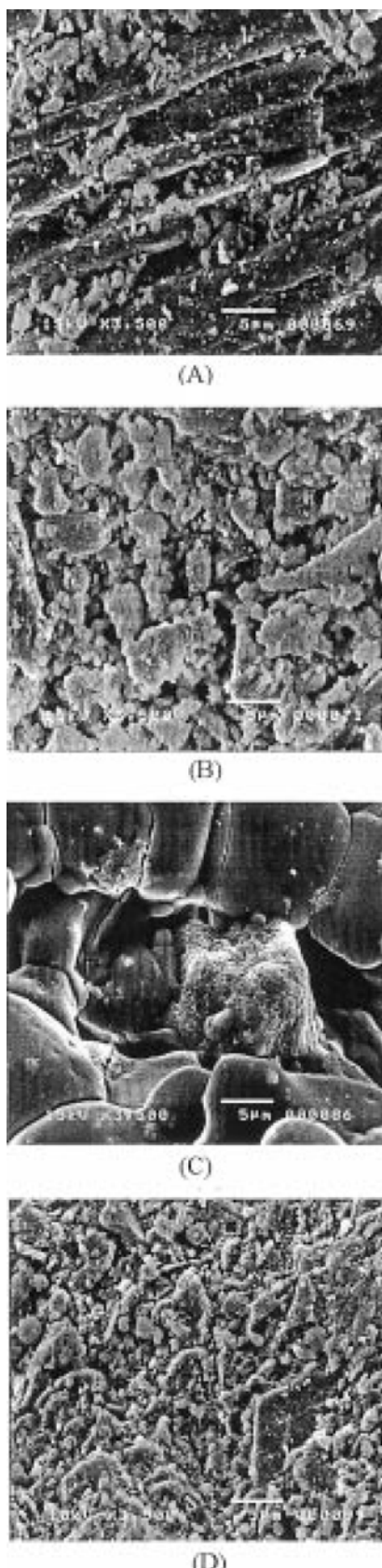


Fig. 8. SEM photographs of calm with a variation of pretreatment condition.

(A) fresh calm, (B) hydrated calm, (C) calcined calm, (D) hydrated after calcination of calm.

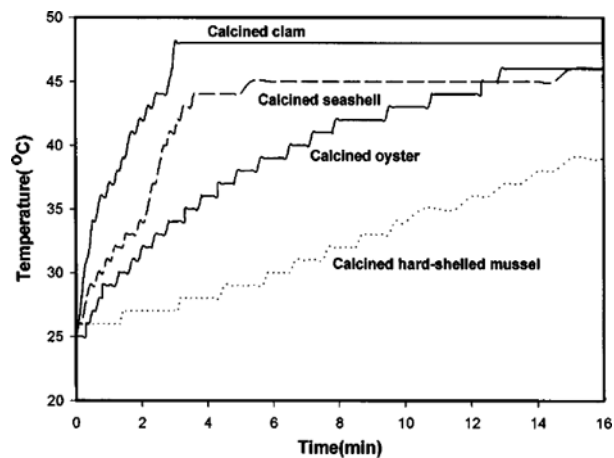


Fig. 9. Variation of sample temperature as a function of hydration time with different absorbents at the starting temperature of 25 °C.

the reactor. When the reaction activity of the sample was checked in the first 3 minutes, calcinated clam was first and then seashell,

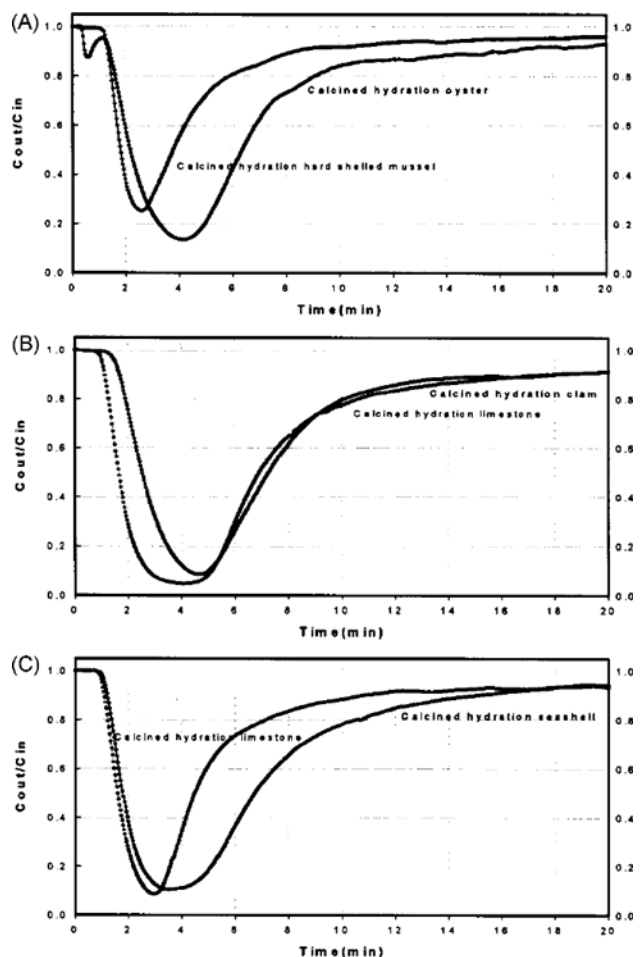


Fig. 10. Variation of SO_2 concentration as a function of reaction time with different absorbents.

(A) hydrated after calcination hard-shelled mussel and oyster, hydrated after calcination clam and limestone, (C) hydrated after calcination seashell and limestone.

oyster. Shiny quicklime was highly increased in the view of the increment of the hydration temperature, but it was the quicklime with low reaction activity. The calcined hard-shelled mussel was also the limestone of low level. When hydrated waste shells and limestone are used in a municipal waste incinerator/power plant SDA process, the retention time of this slurry is about 10-15 seconds so that initial reaction rate is very important. Hard-shell mussel has low reaction activity, but the others could be utilized as good absorbents. Therefore, it can be predicted that calcinated seashell and is more reactive than other sample in the gas removal process. Also, waste shell can be used in powder form. It can be regarded as a good absorbent in an economic aspect, waste recycling. In general, low sulfur coal of 1.5% discharged from a power plant released SO_2 of 1,800-1,900 ppm, O_2 of 6%, CO_2 of 13%, N_2 of 74%, water content of 10%, NO of 600 ppm and HCl of 100 ppm to the air during combustion. The conditions of the research using SO_2 , air and N_2 gas were a reaction temperature of 150 °C, inlet concentration of 1,800 ppm, water content of pseudo-gas of 6 vol%. The removal of organic materials was affected by the forms of absorbent, injected amount, injection temperature, temperature, reaction time, specific surface area, particle size, and polluted gas density in the process which injected absorbent to the burner.

Variation of SO_2 concentration as a function of reaction time

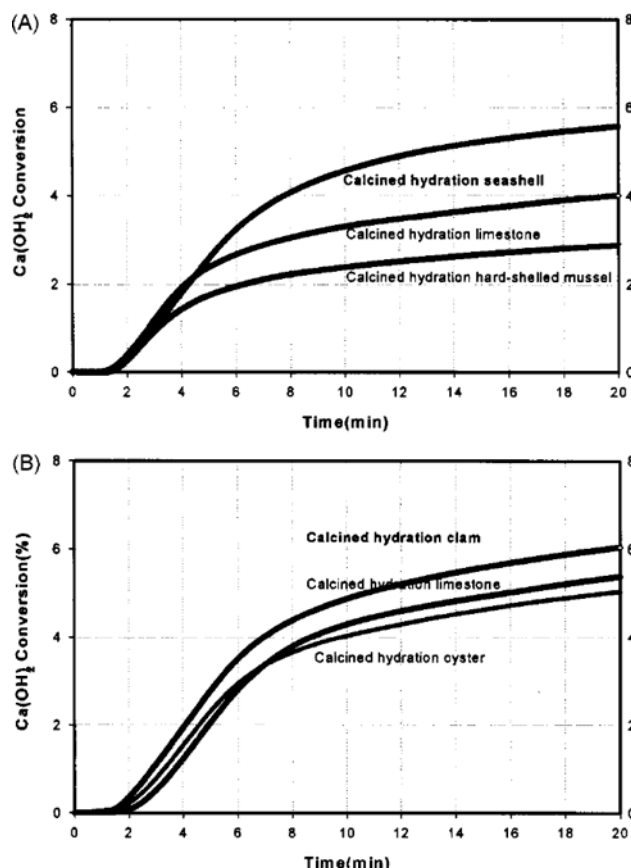


Fig. 11. Variation of conversion of $\text{Ca}(\text{OH})_2$ by sulfation reaction with different absorbents.

(A) hydrated after calcination limestone, seashell, and hard-shelled mussel, (B) hydrated after calcination limestone, clam, and oyster.

with different absorbents has been shown in Fig. 10. This reaction was carried out under the condition of water content of 12.5%, SO_2 concentration of 1,800 ppm, reaction temperature of 15 °C, gas flow of 3 L/min. As sulfation reaction proceeded, outlet SO_2 concentration dropped rapidly due to the formation of calcium sulfite and then reaction was terminated showing a rapid increase of outlet SO_2 concentration after 20 min.

Fig. 11 shows the conversion of waste seashells as a function of reaction time. As shown in Fig. 11, SO_2 removal capacity of clams was best among the tested absorbents. In the case of calcined limestone, the amount of SO_2 removal was recorded to 0.5415 mmole/g. Other shells are as follows: hard-shelled mussel of 0.391 mmole/g, seashell of 0.751 mmole/g, oyster of 0.697 mmole/g. This result implies that most seashells have a comparable desulfurization activity to limestone, except hard-shell mussel. This finding leads to the following conclusion that wastes seashells can be regarded as a good absorbent for removing acid gases. Therefore, recycling the waste seashells as a substitute for limestone would be profitable.

CONCLUSIONS

In this study, the feasibility of using waste seashells as absorbents for the control of air pollution has been investigated in a fixed bed reactor. Physicochemical properties of waste seashells have been characterized by using XRD, SEM, ICP, and BET. Specific surface area of waste seashells increased with increasing reaction temperature when the calcined waste seashells were hydrated. SO_2 removal efficiency of the waste sea shell absorbents after hydration also increased due to the increase of average pore size. The optimum hydration temperature was around 80-90 °C. The order of desulfurization capability of waste seashells was as follows: clam > seashell > oyster > hard-shelled mussel. We can conclude that waste seashells can be used as absorbents for the control of air pollution.

ACKNOWLEDGEMENT

This work was supported by grant No. (1999-30900-001-2) from the University-Industry Collaborative Research program of the Korea Science & Engineering Foundation. The authors thank KOSEF.

REFERENCES

- Acharya, P., DeCicco, S. G. and Novak, R. G., "Factors that Can Influence and Control the Emissions of Dioxins and Furans from Hazardous Waste Incinerators," *J. Air Waste Manage. Assoc.*, **41**(12) (1991).
- Breault, R. W., Litka, A. F., Beittel, R. and Darguzas, J. N., "SO₂ Control in Low Emissions Boiler Systems with the COBRA Process," 1995 SO₂ Control Symposium (1995).
- Brian, K., Jozewicz, W. and Stefanski, L. A., "Reaction Kinetics of Ca-based Sorbents with HCl," *Ind. Eng. Chem. Res.*, **31**(11), 2438 (1992).
- Dahlin, R. S., Snyder, T. R. and Vann Bush, P., "Effects of Sorbent Injection on Particulate Properties part I. Low-Temperature Sorbent Injection," *J. Air Waste Manage. Assoc.*, **42**, 1592 (1992).
- Davini, P., "Thermogravimetric Study of the Characteristics and Re-

activity of CaO Formed in the Presence of Small Amounts of SO₂,” *Fuel*, **74**(7), 995 (1995).

Dempsey, C. R., “A Comparison of Organic Emissions from Hazardous Wasteincinerators Versus the 1990 Toxics Release Inventory Air Releases,” *AIR & WASTE*, **43**, 892 (1993).

EPRI, “FGD Chemistry and Analytical Methods Handbook,” CS-3612 (1988).

Frame, G., “Air Pollution Control Systems for Municipal Solid Waste Incinerators,” *JAPCA*, **38**(8), 1081 (1988).

Jonas Klingspor, K. and Ojerle, I., “Adsorption of Hydrochloric Acid on Solid Slaked Lime for Flue Gas Clean Up,” *Journal of the Air Pollution Control Association*, **31**(11), 1177 (1981).

Jozewicz, W. and Chang, J. C. S., “Evaluation of FGD Dry Injection Sorbents and Additives,” EPA Contract, 68-02-3988 (1989).

Jozewicz, W. and Gullett, B. K., “Structural Transformations in Ca-based Sorbents Used for SO₂ Emission Control, Zement-Kalk-Gips,” **47h**(1), 31 (1994).

Jozewicz, W., Chang, J. C. S., Bma, T. G. and Sedman, C. B., “Reactivation of Solids from Furnace Injection of Limestone for SO₂ Control,” *Environ. Sci. Techno.*, **21**(7), 664 (1987).

Jozewicz, W., Chang, J. C. S., Sedman, C. B. and Bran, T. G., “Characterization of Advanced Sorbents for Dry SO₂ Control,” *Reactivity of Solids*, **6**, 243 (1988).

KIER, “Development of Advanced Technology for Removal of Environmental Pollutants from Flue Gas,” KIER-966405/1 (1996).

Krammer, G., Brunner, C., Khinast, J. and Staudinger, G., “Reaction of Ca(OH)₂ with SO₂ at Low Temperature,” *Ind. Eng. Chem. Res.*, **36**, 1410 (1997).

Lancia, A., Karatza, D., Musmarra, D. and Pepe, F., “Adsorption of Mercuric Chloride from Simulated Incinerator Exhaust Gas by Means of Sorbalit Particles,” *Journal of Chemical Engineering of Japan*, **29**(6), 939 (1996).

Mobley, D. and Chang, J. C. S., “The Adipic Acid Enhanced Limestone Flue Gas Desulfurization Process,” *Journal of the Air Pollution Control Association*, **31**(12), 1249 (1981).

Nakamura, H., Ueno, T., Tatani, A. and Kotake, S., “Pilot-scale Test Results of Simultaneous SO₂ and NO_x Removal Using Powdery Form of LILAC Absorbent,” 1995 SO₂ Control Symposium (1995).

Weast, R. C. and Astle, M. J. “CRC Handbook of Chemistry and Physics,” 66th 220, CRC Press, Boca Raton, Florida (1985).